The Distribution of Lipid Attached Spin Probes in Bilayers: Application to Membrane Protein Topology

Alexander Vogel, Holger A. Scheidt, and Daniel Huster
Junior Research Group "Solid-state NMR Studies of the Structure of Membrane-associated Proteins", Biotechnological-Biomedical Center, Institute of Medical Physics and Biophysics, University of Leipzig, D-04103 Leipzig, Germany

ABSTRACT The distribution of the lipid-attached doxyl electron paramagnetic resonance (EPR) spin label in 1-palmitoyl-2-oleoyl-*sn*-glycero-3-phosphocholine membranes has been studied by ^{1}H and ^{13}C magic angle spinning nuclear magnetic resonance relaxation measurements. The doxyl spin label was covalently attached to the 5th, 10th, and 16th carbons of the *sn*-2 stearic acid chain of a 1-palmitoyl-2-stearoyl-(5/10/16-doxyl)-*sn*-glycero-3-phosphocholine analog. Due to the unpaired electron of the spin label, ^{1}H and ^{13}C lipid relaxation rates are enhanced by paramagnetic relaxation. For all lipid segments the influence of paramagnetic relaxation is observed even at low probe concentrations. Paramagnetic relaxation rates provide a measure for the interaction strength between lipid segments and the doxyl group. Plotted along the membrane director a transverse distribution profile of the EPR probe is obtained. The chain-attached spin labels are broadly distributed in the membrane with a maximum at the approximate chain position of the probe. Both ^{1}H and ^{13}C relaxation measurements show these broad distributions of the doxyl group in the membrane indicating that ^{1}H spin diffusion does not influence the relaxation measurements. The broad distributions of the EPR label result from the high degree of mobility and structural heterogeneity in liquid-crystalline membranes. Knowing the distribution profiles of the EPR probes, their influence on relaxation behavior of membrane inserted peptide and protein segments can be studied by ^{13}C magic angle spinning nuclear magnetic resonance. As an example, the location of Ala residues positioned at three sites of the transmembrane WALP-16 peptide was investigated. All three doxyl-labeled phospholipid analogs induce paramagnetic relaxation of the respective Ala site. However, for well ordered secondary structures the strongest relaxation enhancement is observed for that doxyl group in the closest proximity to the respective Ala. Thus, this approach allows study of membrane insertion of protein segments with respect to the high molecular mobility in liquid-crystalline membranes.

INTRODUCTION

Electron paramagnetic resonance (EPR) and fluorescence probe labeled phospholipid analogs are important tools in structural and cell biology. For many years these lipids have been used to successfully study lipid trafficking, membrane fusion, protein membrane interaction, membrane protein topology, and many other membrane related phenomena (Müller and Herrmann, 2002; Ge and Freed, 1999; Marsh, 2001; Tang et al., 1996; Arnold et al., 1992; Köhler et al., 1997; Davoust et al., 1983b; Matsuzaki et al., 1995; Wimley and White, 2000; London and Feigenson, 1981; Fromherz, 1989; Hughes et al., 2002; London and Ladokhin, 2002). Many different assays allow researchers to study physical quantities such as surface potential, polarity, dipole moments, molecular distances with angstrom resolution, molecular mobility on various timescales, and so on. However, precise knowledge of the location of these probes in the membrane is necessary to interpret the spectroscopic results. For instance, it has been found that the chain-attached fluorescent probe nitrobenzoxadiazole (NBD) is located in the lipid/water interface of a membrane rather than in the unpolar acyl chain region as the molecular structure would suggest (Chattopadhyay and London, 1987). Also, due to the high molecular dynamics of the membrane, the location of the probe should be described by a broad distribution function parallel to the membrane director (Huster et al., 2001b, 2003). The distribution of the NBD probe has a clear maximum at the upper chain/glycerol region but contacts of NBD with lipid headgroups, lower chain segments, and even the termini of the chains do also occur. This at first sight surprising result agrees well with more recent models of the liquid-crystalline lipid bilayer conveyed by latest x-ray (Petrache et al., 1998; White and Wiener, 1996) and nuclear magnetic resonance (NMR) (Huster et al., 1999) studies, as well as molecular dynamics (MD) simulations (Venable et al., 1993). According to these results, the location of lipid segments parallel to the bilayer normal varies by many angstroms due to thermal motions resulting in a high degree of structural heterogeneity. Consequently, lipid-attached probe molecules experience a similar molecular disorder. Unfortunately, many studies involving probe molecules or lipid segments to calculate molecular distances in liquid-crystalline membranes underestimate the tremendous molecular dynamics of the lipid membrane.

Fluorescence probes immersed into a lipid bilayer at different depths have been used to investigate the interaction of membrane-associated peptides with hydrophilic and hydrophobic lipid segments (Kremer et al., 2001). In the current study, we have investigated the transversal membrane distribution of the doxyl EPR probe attached to various

Submitted February 14, 2003, and accepted for publication May 19, 2003.

A. Vogel and H. A. Scheidt contributed equally to this work.

Address reprint requests to Daniel Huster, Institute of Medical Physics and Biophysics, University of Leipzig, Liebigstr. 27, D-04103 Leipzig, Germany. Tel.: +49 (0) 341-97-15706; Fax: +49 (0) 341-97-15709; E-mail: husd@medizin.uni-leipzig.de.

0006-3495/03/09/1691/11 $2.00

lipid acyl chain positions (Fig. 1). Paramagnetic probes or ions are not only used in EPR studies but also in fluorescence quenching assays (Kim and McNamee, 1998; Liu and Deber, 1997; Xu et al., 2001; London and Feigenson, 1981; London and Ladokhin, 2002) or NMR relaxation studies (Pintacuda and Otting, 2002; Bertini et al., 2001; Villalain, 1996) of lipid mixtures, rafts, and soluble or membrane-bound proteins. Recently, paramagnetic O_2 has become a popular molecule to probe membrane immersion depth in bicelles (Prosser et al., 2001, 2000), membrane protein topology in micelles (Luchette et al., 2002), and accessibility of the probe to surface and interior of soluble proteins (Hernandez et al., 2002; Teng and Bryant, 2000). Also, the quenching of the NMR signal of ligand molecules due to binding to the lactose transport protein has been used to study the interaction between the transporter and its ligand (Spooner et al., 1999).

The presence of unpaired electrons has a profound influence on the nuclei in other membrane molecules. Most clearly, an enhanced nuclear spin relaxation is observed, caused by random variation of the electron spin nuclear interactions leading to new pathways of longitudinal and transverse relaxation (Brulet and McConnell, 1975; Peters et al., 1996). The idea of taking advantage of these effects in membrane research is quite old. Already in 1974 the dynamic structure of lipid membranes has been studied using ^{13}C NMR relaxation measurements on sonicated vesicles in the presence of spin-labeled fatty acids (Godici and Landsberger, 1974).

Further, using the effect of paramagnetic relaxation, Gröbner et al. (1999) have suggested a method to use paramagnetic lanthanide ions to investigate the location of membrane-embedded peptides. Resonance lines of peptide segments that are located in the vicinity of the paramagnetic ions, i.e., the aqueous phase, show broadening due to paramagnetic relaxation whereas segments buried in the acyl chain region of the membrane are uninfluenced. This assay is useful to localize surface-associated peptide segments but it lacks resolution within the acyl chain region of the membrane. This gap can be filled by the application of EPR probes (doxyl moiety) that are attached to varying chain positions of phospholipid analogs as suggested in this study.

In this paper, first we have determined the distribution of chain-attached doxyl groups in the liquid-crystalline membrane parallel to the bilayer normal. Similar to NOESY cross-relaxation rates (Huster et al., 1999), paramagnetic relaxation rates provide a measure for the interaction strength between EPR label and lipid segments. Plotted along the membrane normal, the distribution profile of the probe can be obtained. In the second part of the study, we apply this technique to a transmembrane α-helical model peptide and investigate the location of three Ala residues distributed over the helix. To study the topology of rather mobile membrane-associated peptides in liquid-crystalline bilayers by the classical PISEMA (Wu et al., 1994) or spin diffusion approaches (Huster et al., 2002) is more difficult because molecular mobility scales down dipolar couplings, which makes quantitative analysis complicated. Further, our technique only involves simple relaxation time measurements in combination with magic angle spinning (MAS). Thus, we present a simple and efficient approach to study location of membrane-associated peptide segments in lipid membranes.

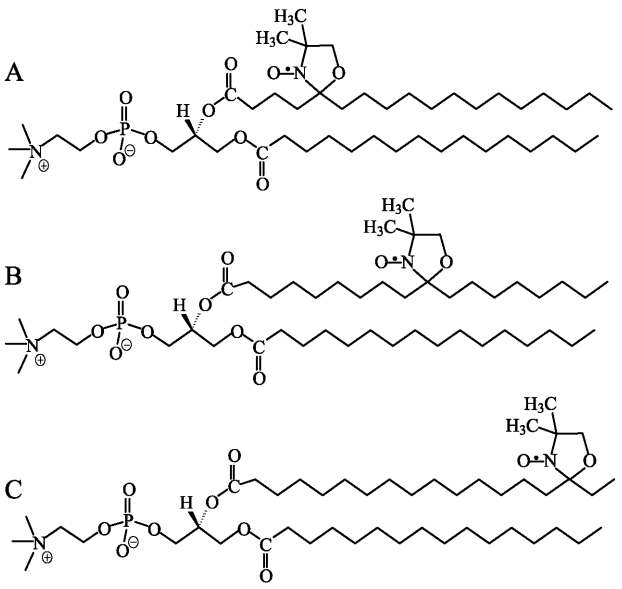

FIGURE 1 Chemical structure of PS-5-doxyl-PC (*A*), PS-10-doxyl-PC (*B*), and PS-16-doxyl-PC (*C*) phospholipid analogs used in this study.

MATERIALS AND METHODS

Materials

1-Palmitoyl-2-stearoyl-(5/10/16-doxyl)-*sn*-glycero-3-phosphocholine (PS-5/10/16-doxyl-PC), 1-palmitoyl-2-oleoyl-*sn*-glycero-3-phosphocholine (POPC), 1-palmitoyl-d_{31}-2-oleoyl-*sn*-glycero-3-phosphocholine (POPC-d_{31}) were purchased from Avanti Polar Lipids, Inc. (Alabaster, AL) and used without further purification. The chemical structures of the three spin-labeled phospholipid analogs are shown in Fig. 1.

Fmoc-[U-^{13}C, ^{15}N]-Ala was purchased from Cambridge Isotopes, Inc. (Cambridge, MA). The WALP-16 peptides with an amino acid sequence of Ac-Gly-Trp-Trp-Leu-Ala-Leu-Ala-Leu-Ala-Leu-Ala-Leu-Ala-Trp-Trp-Ala-$CONH_2$ (Rinia et al., 2000) with the [U-^{13}C, ^{15}N]-Ala in positions 5 and 13 (WALP-16 Ala-5/13), in position 9 (WALP-16 Ala-9), and in position 16 (WALP-16 Ala-16) were synthesized at the Medical Faculty (Charité) of the Humboldt University, Berlin, Germany using standard Fmoc solid phase peptide synthesis.

Sample preparation

Aliquots of lipids were mixed in chloroform and evaporated under a stream of nitrogen. Then, the lipid film was dissolved in ~500 μl cyclohexan, and, after freezing in liquid nitrogen, lyophilizied at a vacuum of ~0.1 mbar resulting in a fluffy lipid powder, which was subsequently hydrated to 40 wt % with deuterium-depleted water for ^2H NMR measurements or D_2O for ^1H NMR measurements. For equilibration, the samples were frozen, thawed, stirred, and gently centrifuged several times. The samples were filled into 5-mm glass vials and sealed for static ^2H NMR experiments. For ^1H MAS

NMR experiments, samples were transferred into 4-mm high-resolution MAS rotors with spherical Kel-F inserts with a volume of ~12 μl.

For the peptide-containing samples, aliquots of spin-labeled lipid analog, POPC, and WALP-16 (2/100/5, mol/mol/mol) were mixed in chloroform, evaporated, and lyophilized as described above. All consecutive preparation steps were carried out as described above. Samples were transferred to 4-mm MAS rotors with cylindrical sample volume and a Teflon insert with a sample volume of ~50 μl. Each sample contained ~3 mg of WALP-16 peptide.

^{1}H and ^{13}C magic-angle spinning NMR

^{1}H MAS spectra were acquired on a DRX600 NMR (Bruker BioSpin, Rheinstetten, Germany) spectrometer operating at a resonance frequency of 600.1 MHz for ^{1}H using a 4-mm high-resolution MAS probe at a spinning speed of 8 kHz and a spectrum width of 10 kHz. Typical $\pi/2$ pulse length was 8 μs. T_1 relaxation times were measured using the inversion recovery pulse sequence with 13 delays between 1 ms and 4 s and a relaxation delay of 4 s.

^{13}C MAS spectra were acquired on a Bruker Avance 750 NMR spectrometer operating at 188.6 MHz for ^{13}C using a double resonance CP MAS probe equipped with a 4-mm spinning module. Single pulse excitation spectra were accumulated at a spectrum width of 60 kHz and a spinning speed of 8 kHz using a $\pi/2$ ^{13}C excitation pulse of a typical length of 6 μs and two pulse phase modulation decoupling (Bennett et al., 1995) at a ^{1}H decoupling field of ~50 kHz. ^{13}C T_1 relaxation times were measured using the inversion recovery pulse sequence with 11 delays between 1 ms and 6–12 s and a relaxation delay of up to 12 s. All NMR measurements were carried out at a temperature of 30°C.

The observed relaxation rates of nuclei in the presence of paramagnetic substances are the sum of the dipolar relaxation rate ($R_{1,D}$), the relaxation rate due to chemical shift anisotropy (CSA, $R_{1,CSA}$), and the paramagnetic relaxation rate ($R_{1,para}$) according to

$$R_1 = R_{1,D} + R_{1,CSA} + R_{1,para}. \quad (1)$$

Although $R_{1,CSA}$ is negligible for ^{1}H NMR, it contributes significantly to the ^{13}C relaxation at higher magnetic field strength. In the absence of paramagnetic probes, the relaxation rate R_1 equals the sum of dipolar and CSA relaxation rates ($R_{1,D}$ + $R_{1,CSA}$). In the presence of spin-labeled phospholipid analogs, the paramagnetic relaxation rate $R_{1,para}$ was determined by subtracting the relaxation rate of the membrane system in the absence of spin label from the relaxation rate in the presence of spin-labeled phospholipid according to Eq. 1.

^{2}H solid-state NMR

^{2}H NMR spectra were recorded on a Bruker DRX300 NMR spectrometer operating at a resonance frequency of 46.1 MHz for ^{2}H using a double channel solids probe equipped with a 5-mm solenoid coil. The ^{2}H spectra were accumulated using a phase-cycled quadrupolar echo sequence (Davis et al., 1976) and a relaxation delay of 0.8 s at a temperature of 30°C. The two 5.8-μs $\pi/2$ pulses were separated by a 100 μs delay. Spectra were left shifted after acquisition to start Fourier transformation on top of the quadrupolar echo. Spectra were dePaked (Sternin et al., 1983) and smoothed order parameter profiles (Lafleur et al., 1989) were determined from the observed quadrupolar splittings ($\Delta\nu_Q$) as described in detail in (Huster et al., 1998).

RESULTS

Distribution of chain-attached doxyl groups in membranes

The presence of phospholipid analogs with a paramagnetic doxyl moiety has a strong influence on the linewidths of the well-resolved ^{1}H MAS NMR spectra due to enhanced nuclear spin relaxation rates. In Fig. 2, representative ^{1}H MAS NMR spectra of POPC with varying concentrations of PS-5-doxyl-PC are shown. In pure POPC spectra, the linewidths vary between ~15 and 40 Hz. Addition of only 1 mol % spin-labeled phospholipids leads to a significant broadening of upper chain and glycerol signals. At a 1:5 molar ratio most signals are broadened beyond the limit of detection by strong paramagnetic transverse relaxation (Fig. 2 *D*). We have also recorded EPR spectra of doxyl-labeled liposomes to confirm that no broadening of EPR spectra due to interactions of probe molecules (Heisenberg exchange) occurs for doxyl concentrations as used in this study (EPR spectra not shown).

More instructively, the influence of the paramagnetic doxyl group on T_1 relaxation times of lipid signals is shown for the terminal CH_3, the glycerol G-1 and the headgroup β segments in dependence on the amount of spin label added in Fig. 3. The presence of the doxyl group leads to a significant

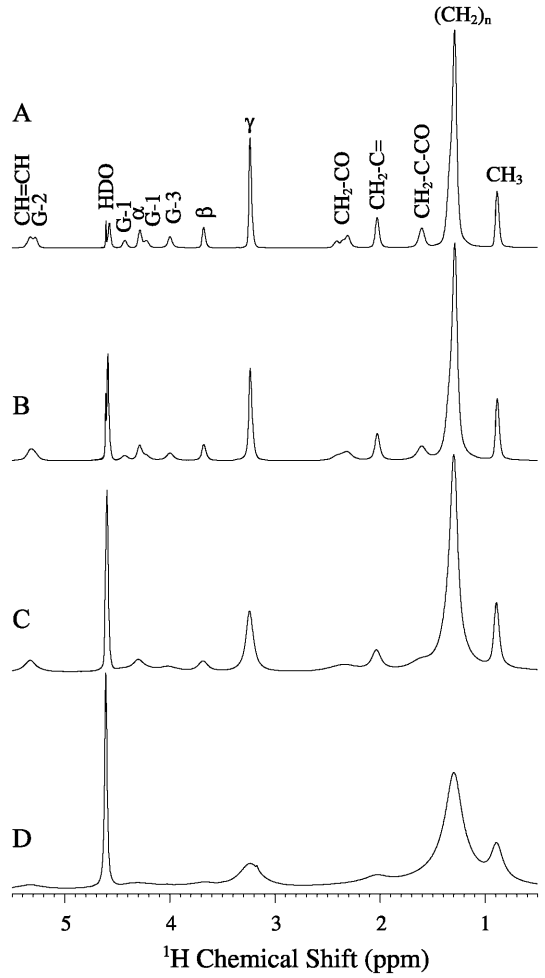

FIGURE 2 600.1 MHz ^{1}H MAS spectra of pure POPC multilamellar vesicles (*A*) and mixtures of POPC/PS-5-doxyl-PC at a molar ratio of 100:1 (*B*), 20:1 (*C*), and 5:1 (*D*) at a temperature of 30°C and a spinning speed of 8 kHz. The samples were hydrated to 40 wt % D_2O.

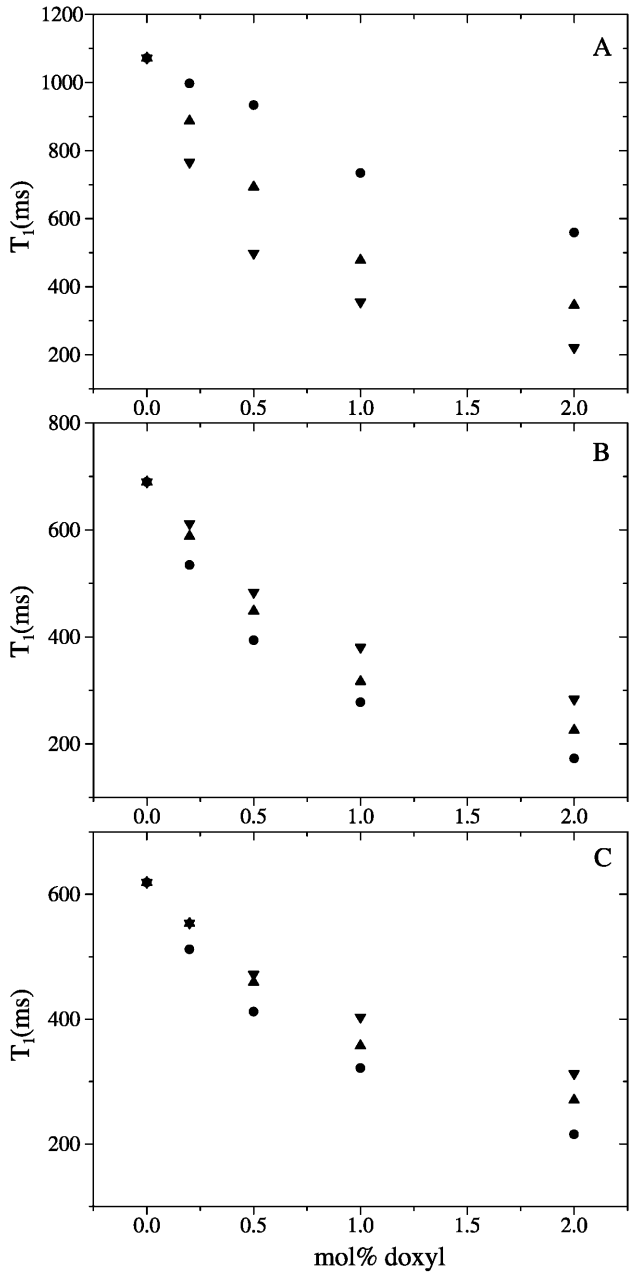

FIGURE 3 600.1 MHz ^{1}H spin lattice relaxation times of POPC segments in the presence of varying concentrations of PS-5-doxyl-PC (●), PS-10-doxyl-PC (▲), and PS-16-doxyl-PC (▼) measured under MAS conditions ($\omega_r/2\pi = 8$ kHz, 30°C). Relaxation times are shown for the terminal $-CH_3$ group (*A*), the G-1 glycerol (*B*), and the β headgroup signals (*C*).

reduction of relaxation times even at concentrations of much less than 1 mol %. However, the reduction of the relaxation time of a certain lipid segment depends strongly on the chain position of the paramagnetic spin probe. For instance, the relaxation time of the terminal CH_3 group is most strongly reduced by PS-16-doxyl-PC and much less by PS-10-doxyl-PC and PS-5-doxyl-PC. Headgroup and glycerol segments are least influenced by PS-16-doxyl-PC, more by PS-10-doxyl-PC, and most by PS-5-doxyl-PC.

These differences can be illustrated best by plotting the paramagnetic relaxation rate of each lipid segment along the membrane normal as shown in Fig. 4 at a molar mixing ratio of 1:200. These plots provide the distribution profile of the EPR probe in the membrane along the normal since paramagnetic relaxation rates are of intermolecular origin and scale with the inverse sixth power of the distance between electron and proton (see Discussion).

The doxyl group attached to the C-5 position of the *sn*-2 chain interacts most strongly with upper chain, glycerol, and headgroup segments of the membrane (Fig. 4 *A*). An interaction of the probe with the middle and lower chain region is possible but occurs less frequently.

If the doxyl probe is attached to the 10th carbon in the *sn*-2 chain, the distribution of the probe has its maximum also in

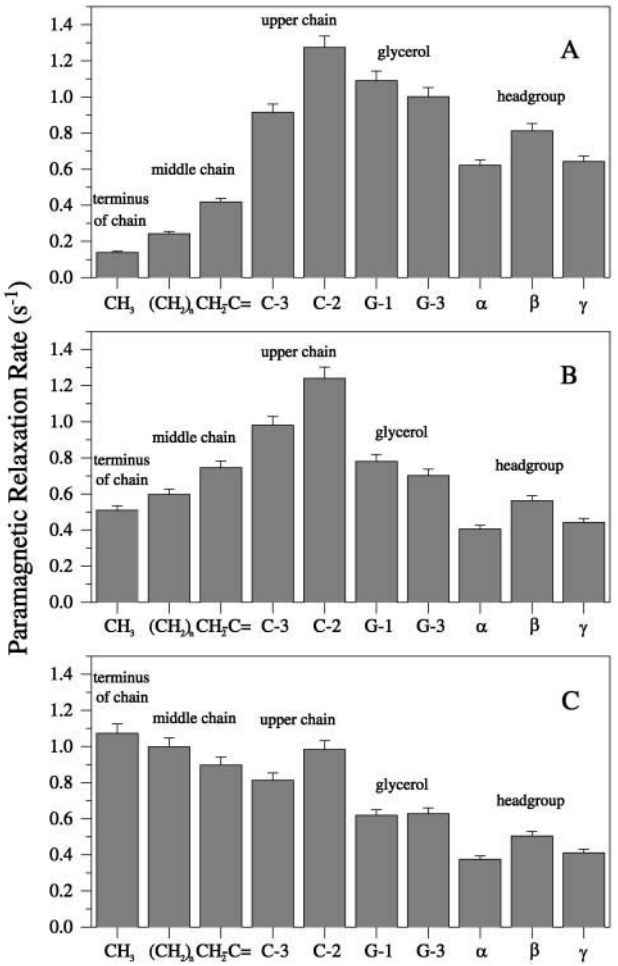

FIGURE 4 600.1 MHz MAS ^{1}H paramagnetic relaxation rates (s^{-1}) of lipid segments in POPC multilamellar vesicles in the presence of PS-5-doxyl-PC (*A*), PS-10-doxyl-PC (*B*), and PS-16-doxyl-PC (*C*) at a molar ratio of 0.5 mol %, a water content of 40 wt %, and a temperature of 30°C. These plots provide a measure for the transverse distribution of the doxyl probes in the membrane.

the upper chain region (Fig. 4 *B*). However, compared to PS-5-doxyl-PC the distribution is biased toward the center of the bilayer.

The probability for the location of the doxyl probe attached to the 16th carbon position in the chain gradually decreases from the chain termini to the headgroup (Fig. 4 *C*). However, there is a finite probability that the spin probe will interact with the headgroup region of the bilayer, most likely by upturning chains.

We have also analyzed ^{13}C NMR paramagnetic relaxation rates at a doxyl probe concentration of 2 mol %, which provide a slightly better resolution in the acyl chain region. These data are shown in Fig. 5. At first sight, good agreement with the ^{1}H relaxation rates is observed. For the PS-5-doxyl-PC and the PS-10-doxyl-PC, the maximum of the distribution is found in the interface region. The distribution for PS-5-doxyl-PC is biased toward the headgroup whereas the distribution of the PS-10-doxyl-PC in POPC is biased toward the middle chain. The distribution of the PS-16-doxyl-PC has its maximum in the lower chain region. Systematically, the paramagnetic relaxation rate for the CO signals is smaller than expected for this region. At the moment, it is not clear what causes this slight discrepancy but it could be related to the accessibility of the doxyl probe to the carbonyl carbons in the highly packed interface region.

As seen in Figs. 4 and 5, all EPR probes are broadly distributed in liquid-crystalline membranes about their position in the acyl chain. The large width of the distribution of the spin probes indicates the transverse mobility and high degree of molecular disorder of the membrane. The observed width of the distribution equals almost one entire membrane leaflet.

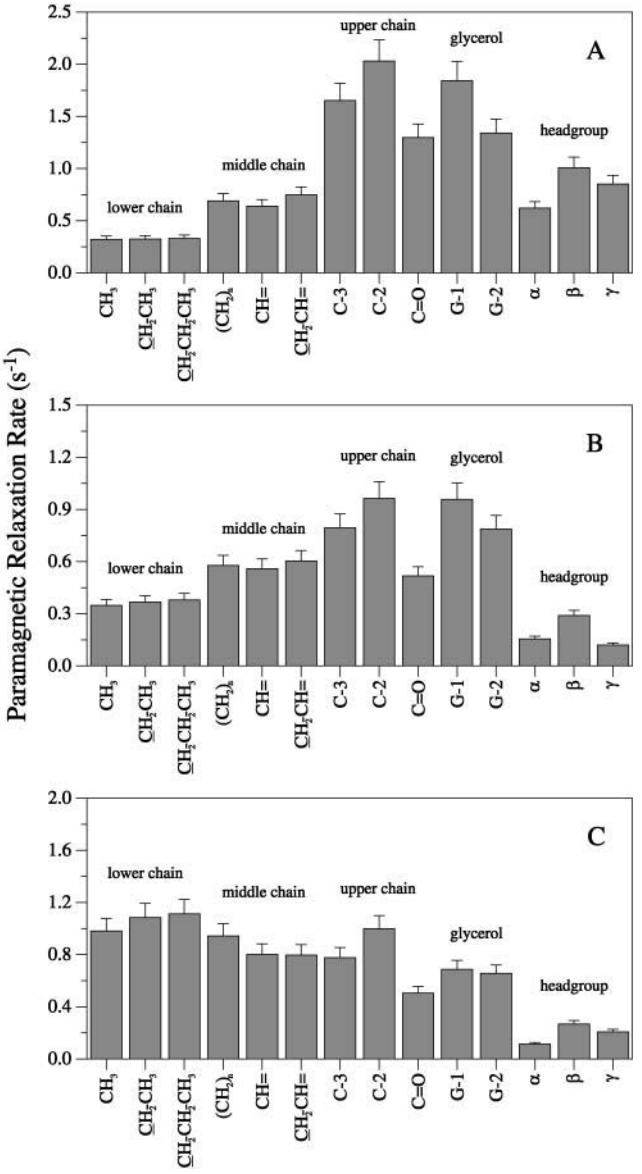

FIGURE 5 188.6 MHz MAS ^{13}C paramagnetic relaxation rates (s^{-1}) of lipid segments in POPC multilamellar vesicles in the presence of 2 mol % PS-5-doxyl-PC (*A*), PS-10-doxyl-PC (*B*), and PS-16-doxyl-PC (*C*) at a water content of 40 wt %, and a temperature of 30°C.

^{2}H NMR order parameters

To investigate the influence of bulky EPR probes on lipid chain packing properties, ^{2}H NMR order parameters of the POPC *sn*-1 chain were studied. ^{2}H NMR spectra of POPC-d_{31} in the presence of the spin-labeled lipids show a slightly increased quadrupolar splitting. To quantify these changes along the hydrophobic chains, order parameter profiles and difference order parameter plots are presented in Fig. 6. The profiles exhibit a moderate increase in chain order in the

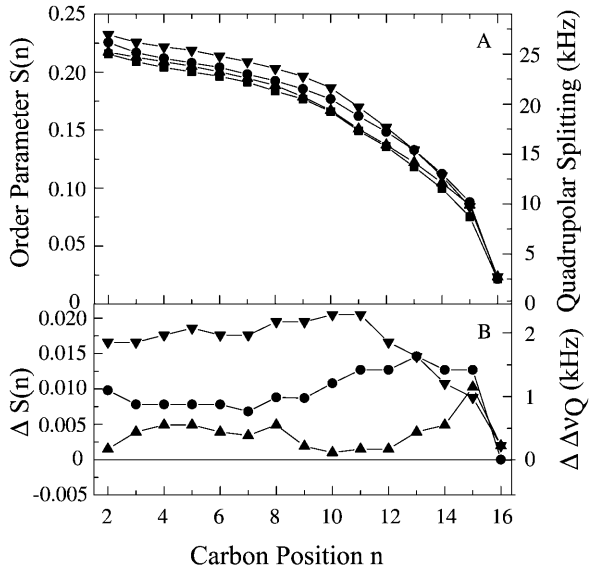

FIGURE 6 Order parameter profiles (*A*) and difference order parameter plots (*B*) for pure POPC (■), POPC/PS-5-doxyl-PC (●), POPC/PS-10-doxyl-PC (▲), and POPC/PS-16-doxyl-PC (▼) at 25 mol % spin-labeled analog. Difference order parameter plots are obtained by subtraction of the order parameter profile of pure POPC-d_{31} from the order parameter profiles of POPC-d_{31} in the presence of the spinlabels.

upper/middle chain region of the membrane for all three spin probes (Fig. 6 *B*).

Such changes are in agreement with a location of the spin probes in the acyl chain region of the membrane and an increase in packing density. The bulky doxyl group occupies a volume of 142 Å^3 which compares with the volume of approximately five CH_2 groups. Thus, the free volume in the membrane is reduced by insertion of the doxyl probe, which decreases the motional freedom of the acyl chains and, therefore, increases chain order parameters. Further, only relative small membrane packing alterations are observed even in the presence of very high concentrations of doxyl-labeled phospholipids. Therefore, the used label concentrations of 1–2 mol % applied for the localization of membrane-embedded peptide segments should not have an influence on lipid packing. Addition of the WALP-16 peptide to POPC membranes at a molar ratio of 1:20 does not result in a modified order parameter profile (data not shown).

Membrane protein topology by paramagnetic relaxation measurements

Paramagnetic spin probes and their influence on the relaxation behavior of membrane-embedded proteins can be investigated to gain structural data. Information about the approximate insertion depth and distribution width of a specific amino acid of a membrane protein can be obtained from relaxation measurements.

In Fig. 7, ^{13}C NMR single pulse excitation spectra of the WALP-16 Ala-16 (*A*) and WALP-16 Ala-9 (*C*) peptides in POPC membranes (1:20, mol/mol) are shown. Besides the narrow signals of highly mobile phospholipids at natural abundance, the ^{13}C signals of labeled Ala are detected. Characteristic differences between the isotropic chemical shift values of the two peptides are observed. Compared to Ala-16, the Cα signal of Ala-9 is shifted downfield, whereas a small upfield shift is observed for the Cβ signal. Absolute chemical shift values for the three WALP-16 peptides are given in Table 1. It has been found that counterdirectional changes of the Cα and Cβ shifts very sensitively indicate secondary structure changes (Spera and Bax, 1991). A downfield shift from the random coil value of the Cα signal with a concomitant upfield shift of the Cβ signal indicates an α-helix structure formation. A clear difference between WALP-16 Ala-9 and Ala-5/13 on the one hand and Ala-16 on the other hand is observed (Table 1) indicating that the C terminus of WALP-16 is unstructured. Addition of doxyl-PC at a molar concentration of 2 mol % only results in a slight broadening of the ^{13}C MAS spectra (see Fig. 7, *B* and *D*).

In the absence of doxyl-labeled lipids the relaxation of these nuclei is due to dipolar and CSA relaxation mechanisms. In the presence of doxyl phospholipid analogs an additional paramagnetic contribution induces fast relaxation of the peptide signals. In Fig. 8, the paramagnetic relaxation rates of the three ^{13}C Ala labeled WALP-16 peptides are plotted at a lipid to peptide molar ratio of 20:1 in the presence of 2 mol % of the spin-labeled phospholipid analogs investigated in this study. Large paramagnetic relaxation rates indicate strong interaction between the doxyl label of the phospholipids and the various Ala residues of the WALP peptides. However, the interaction strength between the different alanines with doxyl groups in various chain positions exhibits characteristic differences.

From the literature it is known that the WALP-16 peptide forms a transmembrane α-helix in lipid membranes (Morein

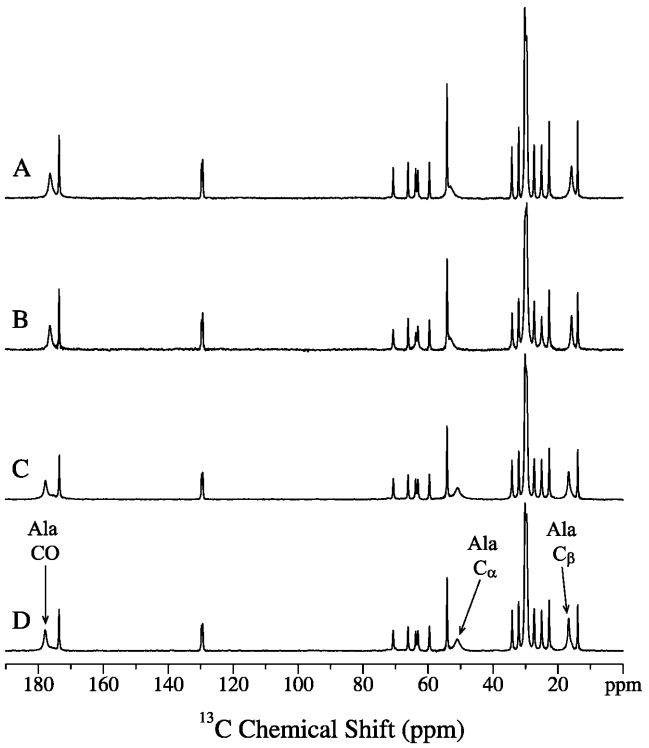

FIGURE 7 Proton decoupled 188.6 MHz ^{13}C MAS spectrum of multilamellar vesicles of POPC/WALP-16 Ala-16 (*A*) and POPC/WALP-16 Ala-9 (*C*) at a lipid/peptide molar ratio of (20:1), a spinning speed of 8 kHz, and a temperature of 30°C. Also, ^{13}C spectra in the presence of 2 mol % doxyl labels for POPC/WALP-16 Ala-16/PS-10-doxyl-PC (*B*), and POPC/WALP-16 Ala-9/PS-10-doxyl-PC (*D*) are shown. The ^{13}C spectra were acquired by single pulse excitation with two pulse phase modulation decoupling ($\gamma B_1/2\pi \approx 50$ kHz). The Ala signals of WALP-16 are assigned according to Cavanagh et al. (1996).

TABLE 1 Isotropic ^{13}C chemical shift values for the Cα and Cβ signals of various alanines in POPC/WALP-16 (20:1, mol/mol) membranes at temperature of 30°C

	δ Cα (ppm)	δ Cβ (ppm)
Ala-9	53.3	15.8
Ala-5/13	52.9	15.6
Ala-16	51.0	16.7

Chemical shift values were referenced to the ^{13}CO signal of Gly (176.4 ppm) used as an external standard.

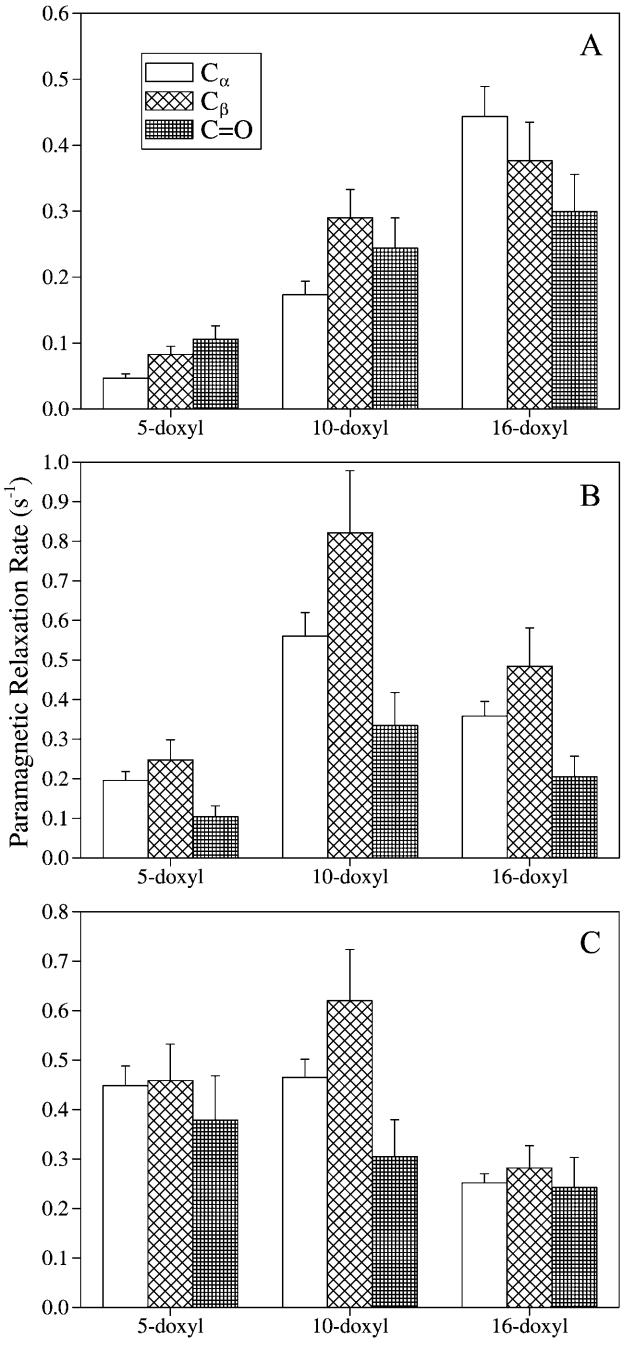

FIGURE 8 188.6 MHz ^{13}C MAS paramagnetic relaxation rates (s^{-1}) of various Ala signals in the WALP-16 peptide incorporated into POPC/doxyl-PC membranes at a water content of 40 wt %, and a temperature of 30°C. (*A*) Ala-9; (*B*) Ala-5/13; (*C*) Ala-16. The molar PS-doxyl-PC/POPC/WALP-16 ratio was 2:100:5, mol/mol/mol.

et al., 1997; de Planque et al., 1998). Therefore, Ala-9 would be located exactly in the middle of the lipid bilayer. As expected for such a system, the paramagnetic relaxation rate of all Ala-9 signals induced by PS-16-doxyl-PC is largest, followed by those of PS-10-doxyl-PC and PS-5-doxyl-PC (Fig. 8 *A*). This indicates that the average position of Ala-9 in WALP-16 is in the middle of the bilayer but also highlights the mobility and high molecular dynamics of the lipid/peptide membrane.

The Ala-5/13 residues of WALP-16 are located four residues above or below the middle of the peptide, respectively. Accordingly, PS-10-doxyl PC induces the strongest paramagnetic relaxation rate consistent with a maximum of the distribution of Ala-5 and 13 in the middle of the hydrocarbon chain of each membrane leaflet (Fig. 8 *B*). Both PS-5-doxyl PC and PS-16-doxyl PC induce lower paramagnetic relaxation rates indicating that these lipid segments have fewer contacts with Ala-5/13 from the WALP-16 peptide. However, the distribution of these amino acids is biased more toward the bilayer center than toward the lipid/water interface.

Finally, Fig. 8 *C* shows the paramagnetic relaxation rates for the C-terminal Ala-16 of the WALP-16 peptide. The maximum of the distribution of Ala-16 must be in the upper half of the hydrocarbon chain as the maximum paramagnetic relaxation rates for this site are induced by PS-5-doxyl PC for CO and by PS-10-doxyl PC for Cβ, whereas the relaxation rates for Cα induced by PS-5-doxyl PC and PS-10-doxyl PC are approximately equal. For all Ala-16 signals, PS-16-doxyl PC induces lower paramagnetic relaxation rates; however, the differences between the paramagnetic relaxation rates induced by three spin labels are relatively small compared to Ala-9 and Ala-5/13.

DISCUSSION

Distribution of EPR probes in liquid-crystalline membranes

Even at low molar concentration, paramagnetic EPR probes enhance relaxation rates of *all* lipid segments of the host matrix. However, this effect is not independent of the chain position of the doxyl label. Therefore, a complete analysis of all lipid relaxation rates provides information about the distribution of the probe in the membrane. Similar to the broad distributions of lipid segments (Huster et al., 1999; Petrache et al., 1998; White and Wiener, 1996), small molecules (Holte and Gawrisch, 1997; Yau et al., 1998; Koeppe et al., 1994; Feller et al., 2002), fluorescence probes (Huster et al., 2001b), or peptides (Huster et al., 2001a; Hristova et al., 2001; Berneche et al., 1998) in liquid-crystalline membranes determined by x ray, NOESY NMR, or MD simulations, the location of spin probes should be described by broad distribution functions. Chain-attached doxyl groups are broadly distributed around the position inferred from a rigid all-*trans* configuration of the acyl chains. Even contacts with the lipid headgroups must occur rather frequently, extending the distribution function of the spin probe over one entire membrane leaflet. The width of the distribution of the doxyl groups is identical for ^{1}H and ^{13}C relaxation measurements indicating that the influence of spin diffusion in the proton network can be excluded.

It is interesting to note that the paramagnetic relaxation rate of the β headgroup protons is systematically larger than that of the α and γ protons for all three phospholipid analogs studied (Figs. 4 and 5). This suggests that the β methylene group of the PC headgroup faces the membrane interior more frequently than the α and γ protons. Indeed, a slight preference for this orientation of C-H bonds in the headgroup has been seen in MD simulations (S. E. Feller, (Wabash College, Crawfordsville, IN, personal communication).

The dominant factor, describing the relaxation of a nuclear spin in the presence of a paramagnetic probe due to dipolar interaction between electron and nucleus is their distance (Vega and Fiat, 1976; Brulet and McConnell, 1975). As in all dipolar relaxation phenomena, the relaxation rate is proportional to r^{-6}, r being the (fixed) distance between nucleus and unpaired electron, if the vector between electron and nuclear spin undergoes isotropic motions, which appears to be a reasonable approximation in liquid-crystalline membranes (Feller et al., 1999). The inverse sixth-power distance dependence of the paramagnetic relaxation rate suggests that the influence of the electron spin on nuclear relaxation is largely confined to the segments of closest approach. Alternatively, diffusional relaxation models can be invoked to explain nuclear relaxation in the presence of paramagnetic nitroxides (Brulet and McConnell, 1975; Polnaszek and Bryant, 1984). In these models, the lipids and spin label diffuse relative to one another, which modulates the dipolar energy resulting in relaxation. This leads to an enhancement of nuclear relaxation that also strongly depends on the intermolecular distance between electron and nuclear spin. Therefore, the long-distance correlations of spin label and molecular segments of phospholipid molecules or peptides must be due to direct contacts caused by the molecular disorder in the lipid membrane.

Recently, distribution functions of small molecules in membranes were determined by NOESY cross-relaxation rate analysis (Holte and Gawrisch, 1997; Yau et al., 1998). Because of their strong internuclear distance dependence, cross-relaxation rates represent a measure for the relative interaction strengths between the participating protons (Feller et al., 2002). Since the same distance dependence applies for the paramagnetic relaxation rates they may also be interpreted as a measure for the contact probability between electron and nuclear spins.

It should be noted that due to the much stronger magnetic moment of the electron spin, nuclear relaxation is affected up to distances of ~25 Å (Prosser et al., 2001). However, due to the strong inverse distance dependence enhancement of nuclear relaxation rates strongly decreases with distance. Therefore, only the contacts with the shortest distance contribute significantly (Brulet and McConnell, 1975).

Our results for paramagnetic relaxation rates of lipid segments in the presence of a spin probe agree with previous measurements of spin-labeled fatty acids in sonicated vesicles, (Godici and Landsberger, 1974; Ellena et al., 1988). Therefore, it can be concluded that the distribution width of doxyl groups attached to phospholipid chains is not different from those attached to free fatty acids.

Similar to the distribution of the fluorescence probe NBD, chain-attached doxyl groups show a broad distribution in the membrane. However, the presence of a doxyl group does not cause backfolding of the entire chain as observed for NBD (Chattopadhyay and London, 1987). In spite of their similar size the NBD moiety possesses fixed charges whereas the doxyl group is uncharged, which probably explains the different location of the probes. Although NBD most favorably interacts with the complicated electrostatic structure of the lipid/water interface of the membrane, the relatively unpolar doxyl groups remain in the hydrophobic acyl chain region of the membrane where they experience attractive van der Waals interactions. Since the inherent disorder and high mobility of the lipid acyl chain region in the liquid-crystalline phase state has been well established in spectroscopic studies (Huster and Gawrisch, 2000; White and Wiener, 1996) and MD simulations (Venable et al., 1993; Feller et al., 1999) this investigation underlines that small probe molecules attached to the lipid chains are subject to the same dynamics and high mobility. In other words, the distribution of chain-attached probe molecules in liquid-crystalline membranes is as chaotic as the entire acyl chain region. This high mobility also allows to neglect the effects of spin diffusion in these measurements (Huster and Gawrisch, 1999). This is confirmed by our results because the distribution profiles of doxyl measured by ^{1}H and ^{13}C MAS NMR are very similar. A quantitative distinction between the contributions from the width of the doxyl distribution versus the chain upturns and headgroup mobility cannot be made on the basis of the NMR relaxation measurements. However, a promising tool for better understanding the large variety of dynamic lipid structures and conformations is MD simulations, which can help to address this issue (Feller et al., 2002).

Investigation of membrane peptide topology

After determining the dynamic relocalization and width of the distribution of chain-attached doxyl spin labels in the membrane the question arises whether these broadly distributed probes are useful for the study of insertion depth of membrane-bound peptides and membrane protein segments by EPR or fluorescence spectroscopy (Liu and Deber, 1997; Kim and McNamee, 1998; Davoust et al., 1983a) or NMR methods as suggested in this study.

Even though the doxyl groups show a very broad distribution a relatively well defined maximum is found for each probe. It has to be realized that the relative location of the mobile doxyl group is measured with regard to the mobile lipid segments, which may also bias the width of the distribution. Membrane-bound peptides and proteins repre-

sent more rigid structures compared to lipid molecules. However, even for membrane-associated peptides or membrane protein segments it is necessary to consider distribution rather then fixed location as suggested by White and coworkers (White et al., 2001).

We have used the transmembrane WALP-16 peptide as a model to investigate spatial resolution of spin probe quenching. The topology of membrane spanning WALP-16 is well known (Morein et al., 1997; de Planque et al., 1998). For instance, Ala-9 should be located in the middle of the bilayer. In agreement with that topology, our relaxation measurements indicate that Ala-9 interacts strongest with PS-16-doxyl-PC, weaker with PS-10-doxyl-PC, and to the smallest extent with PS-5-doxyl-PC (Fig. 8 *A*). The second peptide investigated was WALP-16 Ala-5/13 (Fig. 8 *B*). Here, the ^{13}C Ala labels are located equally distant from Ala-9 at the peptide center. If one assumes an ideal helix with a translation of 1.5 Å per residue (Creighton, 1993), these labels are located 6 Å above or below Ala-9. Accordingly, highest paramagnetic relaxation rates are observed for PS-10-doxyl-PC. This places Ala-5/13 approximately in the middle of the hydrocarbon chains of each membrane leaflet.

As inferred from the isotropic chemical shift measurements, Ala-9 and Ala-5/13 are located in a well defined α-helix whereas Ala-16 resides in the unstructured C terminus (Table 1). Accordingly, the distribution width of Ala-16 is much broader, having a maximum in the upper chain region. Ala-16 is preceded by two Trp residues which have been shown to preferentially localize in the lipid/water interface of the membrane (Yau et al., 1998; Persson et al., 1998). Apparently, the C terminus of WALP-16 acquires significant molecular mobility as its distribution is broader than for the other two positions that are located in a rather stiff helix arrangement (Fig. 8 *C*).

The location of the Ala-16 residue of WALP-16 cannot be determined unambiguously as the Cβ signal shows strongest paramagnetic relaxation rates for PS-10-doxyl-PC, the CO signal exhibits strongest paramagnetic relaxation data for PS-5-doxyl-PC, and for the Cα signal the paramagnetic relaxation rates for PS-5-doxyl-PC and PS-10-doxyl-PC are equal. However, the differences in the paramagnetic relaxation rates for Ala-16 induced by 5-doxyl and 10-doxyl are within experimental error of the relaxation measurement. Ala-16 is difficult to localize because the distributions of 5-doxyl and 10-doxyl in the bilayers show an appreciable superposition. The membrane interface is defined as a broad region of ~10–15 Å width. The nonstructured C terminus of WALP-16 is localized within this region and, therefore, the paramagnetic relaxation rates induced by 5-doxyl and 10-doxyl are indistinguishable within experimental error. Therefore, it is concluded that the C terminus of the WALP-16 peptide is mobile and distributed in the lipid/water interface of the membrane.

These results impose two important conclusions: First, interactions between lipid-attached probes and molecular segments of membrane proteins have to be interpreted with regard to the thermal motions and molecular disorder of the lipid membrane. An interpretation of these interactions in terms of distances with a resolution of fractions of angstroms is not appropriate. Rather, membrane-associated peptides and even membrane protein segments are subject to fast molecular dynamics, which requires a description of their location parallel to the membrane normal by broad distribution functions. Second, lipid-attached EPR probes are useful tools to study the location of membrane protein segments in terms of the distribution of these segments parallel to the bilayer normal. However, a meaningful measurement requires study of at least three different chain locations of EPR probes. From the difference between the effects of deeply inserted quenchers and those of more shallowly located quenchers an approximate location of the membrane protein site can be determined. This allows the use of EPR probes to study location of membrane-inserted protein segments supplementary to utilizing paramagnetic ions, which are more practical for studying location of surface-associated protein segments (Gröbner et al., 1999).

The advantage of using NMR to study the location of membrane protein segments by paramagnetic relaxation due to EPR probes is that through specific isotopic labeling any given segment of a membrane protein can be investigated. This allows investigation of wildtype proteins rather than tryptophan, fluorine, or fluorescence-labeled mutants. As seen from the ^{2}H NMR experiments, membrane structure is influenced by bulky EPR probes; however, only low probe concentrations of 2 mol % or less are required, making this NMR methodology a useful strategy to study membrane protein topology.

Recently, the application of gradients of paramagnetic O_2 has been introduced as a new method to study membrane protein topology and the immersion depth of protein segments into micelles (Luchette et al., 2002). Although the big advantage of this method is that molecular O_2 should not have an influence on acyl chain packing, the technical requirements for the application of high oxygen pressure on the order of 100 atm prohibits the application of MAS and thus restricts the investigation to solution NMR applications. With the doxyl spin probe method described here, solid-state NMR experiments can be carried out, which means that membrane proteins can be investigated in lipid bilayers and that there is no principal size limitation of the investigated protein.

The authors gratefully acknowledge valuable discussions with Dr. Klaus Gawrisch. The authors thank Lars Thomas for technical assistance with EPR measurements. D.H. thanks Dr. Heiko Scherf and Felix Böllmann for support with the measurements.

The junior research group is funded by the Saxon State Ministry of Higher Education, Research and Culture.

REFERENCES

Arnold, K., D. Hoekstra, and S. Ohki. 1992. Association of lysozyme to phospholipid surfaces and vesicle fusion. *Biochim. Biophys. Acta.* 1124:88–94.

Bennett, A. E., C. M. Rienstra, M. Auger, K. V. Lakshmi, and R. G. Griffin. 1995. Heteronuclear decoupling in rotating solids. *J. Chem. Phys.* 103:6951–6958.

Berneche, S., M. Nina, and B. Roux. 1998. Molecular dynamics simulation of melittin in a dimyristoylphosphatidylcholine bilayer membrane. *Biophys. J.* 75:1603–1618.

Bertini, I., C. Luchinat, and M. Piccioli. 2001. Paramagnetic probes in metalloproteins. *Methods Enzymol.* 339:314–340.

Brulet, P., and H. M. McConnell. 1975. Magnetic resonance spectra of membranes. *Proc. Natl. Acad. Sci. USA.* 72:1451–1455.

Cavanagh, J., W. J. Fairbrother, A. G. Palmer III, and N. J. Skelton. 1996. Protein NMR Spectroscopy. Principles and Practice. Academic Press, San Diego.

Chattopadhyay, A., and E. London. 1987. Parallax method for direct measurement of membrane penetration depth utilizing fluorescence quenching by spin-labeled phospholipids. *Biochemistry.* 26: 39–45.

Creighton, T. E. 1993. Proteins. Structures and Molecular Properties. W. H. Freeman and Company, New York.

Davis, J. H., K. R. Jeffrey, M. Bloom, M. I. Valic, and T. P. Higgs. 1976. Quadrupolar echo deuteron magnetic resonance spectroscopy in ordered hydrocarbon chains. *Chem. Phys. Lett.* 42:390–394.

Davoust, J., M. Seigneuret, P. Herve, and P. F. Devaux. 1983a. Collisions between nitrogen-14 and nitrogen-15 spin-labels. 1. Lipid-lipid interactions in model membranes. *Biochemistry.* 22:3137–3145.

Davoust, J., M. Seigneuret, P. Herve, and P. F. Devaux. 1983b. Collisions between nitrogen-14 and nitrogen-15 spin-labels. 2. Investigations on the specificity of the lipid environment of rhodopsin. *Biochemistry.* 22: 3146–3151.

de Planque, M. R., D. V. Greathouse, R. E. Koeppe 2nd, H. Schafer, D. Marsh, and J. A. Killian.1998. Influence of lipid/peptide hydrophobic mismatch on the thickness of diacylphosphatidylcholine bilayers. A ^{2}H NMR and ESR study using designed transmembrane alpha-helical peptides and gramicidin A. *Biochemistry.* 37:9333–9345.

Ellena, J. F., S. J. Archer, R. N. Dominey, B. D. Hill, and D. S. Cafiso. 1988. Localizing the nitroxide group of fatty acid and voltage-sensitive spin-labels in phospholipid bilayers. *Biochim. Biophys. Acta.* 940:63–70.

Feller, S. E., C. A. Brown, D. T. Nizza, and K. Gawrisch. 2002. Nuclear Overhauser enhancement spectroscopy cross-relaxation rates and ethanol distribution across membranes. *Biophys. J.* 82:1396–1404.

Feller, S. E., D. Huster, and K. Gawrisch. 1999. Interpretation of NOESY cross-relaxation rates from molecular dynamics simulations of a lipid bilayer. *J. Am. Chem. Soc.* 121:8963–8964.

Fromherz, P. 1989. Lipid coumarin dye as a probe of interfacial electrical potential in biomembranes. *Methods Enzymol.* 171:376–387.

Ge, M., and J. H. Freed. 1999. Electron-spin resonance study of aggregation of gramicidin in dipalmitoylphosphatidylcholine bilayers and hydrophobic mismatch. *Biophys. J.* 76:264–280.

Godici, P. E., and F. R. Landsberger. 1974. The dynamic structure of lipid membranes. A ^{13}C nuclear magnetic resonance study using spin labels. *Biochemistry.* 13:362–368.

Gröbner, G., C. Glaubitz, and A. Watts. 1999. Probing membrane surfaces and the location of membrane-embedded peptides by ^{13}C MAS NMR using lanthanide ions. *J. Magn. Reson.* 141:335–339.

Hernandez, G., C. L. Teng, R. G. Bryant, and D. M. LeMaster. 2002. O_2 penetration and proton burial depth in proteins: applicability to fold family recognition. *J. Am. Chem. Soc.* 124:4463–4472.

Holte, L. L., and K. Gawrisch. 1997. Determining ethanol distribution in phospholipid multilayers with MAS-NOESY spectra. *Biochemistry.* 36:4669–4674.

Hristova, K., C. E. Dempsey, and S. H. White. 2001. Structure, location, and lipid perturbations of melittin at the membrane interface. *Biophys. J.* 80:801–811.

Hughes, W. E., B. Larijani, and P. J. Parker. 2002. Detecting protein-phospholipid interactions. Epidermal growth factor-induced activation of phospholipase D1b in situ. *J. Biol. Chem.* 277:22974–22979.

Huster, D., K. Arnold, and K. Gawrisch. 1998. Influence of docosahexaenoic acid and cholesterol on lateral lipid organization in phospholipid membranes. *Biochemistry.* 37:17299–17308.

Huster, D., K. Arnold, and K. Gawrisch. 1999. Investigation of lipid organization in biological membranes by two-dimensional nuclear Overhauser enhancement spectroscopy. *J. Phys. Chem. B.* 103:243–251.

Huster, D., and K. Gawrisch. 1999. NOESY NMR crosspeaks between lipid headgroups and hydrocarbon chains: spin diffusion or molecular disorder? *J. Am. Chem. Soc.* 121:1992–1993.

Huster, D., and K. Gawrisch. 2000. New insights into biomembrane structure from two-dimensional nuclear Overhauser enhancement spectroscopy. *In* Lipid Bilayers: Structure and Interactions. J. Katsaras and T. Gutberlet, editors. Springer Verlag, Berlin, Germany. 109–25.

Huster, D., K. Kuhn, D. Kadereit, H. Waldmann, and K. Arnold. 2001a. High resolution magic angle spinning NMR for the investigation of a *ras* lipopeptide in a lipid bilayer. *Angew. Chem. Intl. Ed.* 40:1056–1058.

Huster, D., P. Müller, K. Arnold, and A. Herrmann. 2001b. Dynamics of membrane penetration of the fluorescent 7-nitrobenz-2-oxa-1,3-diazol-4-yl (NBD) group attached to an acyl chain of phosphatidylcholine. *Biophys. J.* 80:822–831.

Huster, D., X. Yao, and M. Hong. 2002. Membrane protein topology probed by ^{1}H spin diffusion from lipids using solid-state NMR spectroscopy. *J. Am. Chem. Soc.* 124:874–883.

Huster, D., P. Müller, K. Arnold, and A. Herrmann. 2003. The distribution of chain attached 7-nitrobenz-2oxa-1,3-diazol-4-yl (NBD) in acidic membranes determined by ^{1}H MAS NMR spectroscopy. *Eur. Biophys. J.* 32:47–54.

Kim, J., and M. G. McNamee. 1998. Topological disposition of Cys 222 in the alpha-subunit of nicotinic acetylcholine receptor analyzed by fluorescence-quenching and electron paramagnetic resonance measurements. *Biochemistry.* 37:4680–4686.

Koeppe, R. E 2nd., J. A. Killian, and D. V. Greathouse. 1994. Orientations of the tryptophan 9 and 11 side chains of the gramicidin channel based on deuterium nuclear magnetic resonance spectroscopy. *Biophys. J.* 66:14–24.

Köhler, G., U. Hering, O. Zschörnig, and K. Arnold. 1997. Annexin V interaction with phosphatidylserine-containing vesicles at low and neutral pH. *Biochemistry.* 36:8189–8194.

Kremer, J. J., D. J. Skansky, and R. M. Murphy. 2001. Profile of changes in lipid bilayers structure caused by β-amyloid peptide. *Biochemistry.* 40:8563–8571.

Lafleur, M., B. Fine, E. Sternin, P. R. Cullis, and M. Bloom. 1989. Smoothed orientational order profile of lipid bilayers by ^{2}H-nuclear magnetic resonance. *Biophys. J.* 56:1037–1041.

Liu, L. P., and C. M. Deber. 1997. Anionic phospholipids modulate peptide insertion into membranes. *Biochemistry.* 36:5476–5482.

London, E., and G. W. Feigenson. 1981. Fluorescence quenching in model membranes. 2. Determination of local lipid environment of the calcium adenosinetriphosphatase from sarcoplasmic reticulum. *Biochemistry.* 20:1939–1948.

London, E., and A. S. Ladokhin. 2002. Measuring the depth of amino acid residues in membrane-inserted peptides by fluorescence quenching. *In* Current Topics in Membranes. S. A. Simon and T. J. McIntosh, editors. Elsevier Science, Amsterdam, The Netherlands. 89–115.

Luchette, P. A., R. S. Prosser, and C. R. Sanders. 2002. Oxygen as a paramagnetic probe of membrane protein structure by cysteine mutagenesis and (19)F NMR spectroscopy. *J. Am. Chem. Soc.* 124:1778–1781.

Marsh, D. 2001. Polarity and permeation profiles in lipid membranes. *Proc. Natl. Acad. Sci. USA.* 98:7777–7782.

Matsuzaki, K., O. Murase, N. Fujii, and K. Miyajima. 1995. Translocation of a channel-forming antimicrobial peptide, magainin 2, across lipid bilayers by forming a pore. *Biochemistry.* 34:6521–6526.

Morein, S., E. Strandberg, J. A. Killian, S. Persson, G. Arvidson, R. E. Koeppe 2nd, and G. Lindblom. 1997. Influence of membrane-spanning alpha-helical peptides on the phase behavior of the dioleoylphosphatidylcholine/water system. *Biophys. J.* 73:3078–3088.

Müller, P., and A. Herrmann. 2002. Rapid transbilayer movement of spin-labeled steroids in human erythrocytes and in liposomes. *Biophys. J.* 82:1418–1428.

Persson, S., J. A. Killian, and G. Lindblom. 1998. Molecular ordering of interfacially localized tryptophan analogs in ester- and ether-lipid bilayers studied by ^{2}H-NMR. *Biophys. J.* 75:1365–1371.

Peters, J. A., J. Huskens, and D. J. Raber. 1996. Lanthanide induced shifts and relaxation rate enhancements. *Prog. Nucl. Magn. Reson. Spectrosc.* 28:283–350.

Petrache, H. I., N. Gouliaev, S. Tristram-Nagle, R. Zhang, R. M. Suter, and J. F. Nagle. 1998. Interbilayer interactions from high resolution x-ray scattering. *Phys. Rev. E.* 57:7014–7024.

Pintacuda, G., and G. Otting. 2002. Identification of protein surfaces by NMR measurements with a paramagnetic Gd(III) chelate. *J. Am. Chem. Soc.* 124:372–373.

Polnaszek, C. F., and R. G. Bryant. 1984. Nitroxide radical induced solvent proton relaxation: measurement of localized translational diffusion. *J. Chem. Phys.* 81:4038–4045.

Prosser, R. S., P. A. Luchette, and P. W. Westerman. 2000. Using O_2 to probe membrane immersion depth by 19F NMR. *Proc. Natl. Acad. Sci. USA.* 97:9967–9971.

Prosser, R. S., P. A. Luchette, P. W. Westerman, A. Rozek, and R. E. Hancock. 2001. Determination of membrane immersion depth with O_2: a high-pressure ^{19}F NMR study. *Biophys. J.* 80:1406–1416.

Rinia, H. A., R. A. Kik, R. A. Demel, M. M. Snel, J. A. Killian, J. P. Der Eerden, and B. de Kruijff. 2000. Visualization of highly ordered striated domains induced by transmembrane peptides in supported phosphatidylcholine bilayers. *Biochemistry.* 39:5852–5858.

Spera, S., and A. Bax. 1991. Empirical correlation between protein backbone conformation and Cα and Cβ ^{13}C nuclear magnetic resonance chemical shifts. *J. Am. Chem. Soc.* 113:5490–5492.

Spooner, P. J. R., L. M. Veenhoff, A. Watts, and B. Poolman. 1999. Structural information on a membrane transport protein from nuclear magnetic resonance spectroscopy using sequence-selective nitroxide labeling. *Biochemistry.* 38:9634–9639.

Sternin, E., M. Bloom, and L. MacKay. 1983. De-Pake-ing of NMR spectra. *J. Magn. Reson.* 55:274–282.

Tang, X. J., M. S. Halleck, R. A. Schlegel, and P. Williamson. 1996. A subfamily of P-type ATPases with aminophospholipid transporting activity. *Science.* 272:1495–1497.

Teng, C. L., and R. G. Bryant. 2000. Experimental measurement of nonuniform dioxygen accessibility to ribonuclease A surface and interior. *J. Am. Chem. Soc.* 122:2667–2668.

Vega, A. J., and D. Fiat. 1976. Nuclear relaxation processes of paramagnetic complexes. The slow-motion case. *Mol. Phys.* 31:347–355.

Venable, R. M., Y. Zhang, B. J. Hardy, and R. W. Pastor. 1993. Molecular dynamics simulations of a lipid bilayer and of hexadecane: an investigation of membrane fluidity. *Science.* 262:223–226.

Villalain, J. 1996. Location of cholesterol in model membranes by magic-angle-sample-spinning NMR. *Eur. J. Biochem.* 241:586–593.

White, S. H., A. S. Ladokhin, S. Jayasinghe, and K. Hristova. 2001. How membranes shape protein structure. *J. Biol. Chem.* 276:32395–32398.

White, S. H., and M. C. Wiener. 1996. The liquid-crystallographic structure of fluid lipid bilayer membranes. *In* Biological Membranes. A Molecular Perspective from Computation and Experiment. K. M. Merz and B. Roux, editors. Birkhäuser, Boston, MA. 127–144.

Wimley, W. C., and S. H. White. 2000. Determining the membrane topology of peptides by fluorescence quenching. *Biochemistry.* 39:161–170.

Wu, C. H., A. Ramamorthy, and S. J. Opella. 1994. High-resolution heteronuclear dipolar solid-state NMR spectroscopy. *J. Magn. Reson. A.* 109:270–272.

Xu, X., R. Bittman, G. Duportail, D. Heissler, C. Vilcheze, and E. London. 2001. Effect of the structure of natural sterols and sphingolipids on the formation of ordered sphingolipid/sterol domains (rafts). Comparison of cholesterol to plant, fungal, and disease-associated sterols and comparison of sphingomyelin, cerebrosides, and ceramide. *J. Biol. Chem.* 276:33540–33546.

Yau, W. M., W. C. Wimley, K. Gawrisch, and S. H. White. 1998. The preference of tryptophan for membrane interfaces. *Biochemistry.* 37:14713–14718.